SCIENTIFIC PAPER
Published: November 28, 2025
https://doi.org/10.13167/2025.31.13

Implementation of a substructure method to analyse soil-structure interaction at an existing 10-storey reinforced concrete building

Besar Abdiu[1,2]✉, Julijana Bojadjieva[2], Aleksandra Bogdanovic[2], Antonio Shoklarovski[2], Kemal Edip[2] and Vlatko Sheshov[2]

[1] Mother Teresa University, Faculty of Civil Engineering and Architecture, Street 1669, 11A, 1010, Skopje, North Macedonia

[2] Ss. Cyril and Methodius, Institute of Earthquake Engineering and Engineering Seismology, Todor Aleksandrov, 165, 1000, Skopje, North Macedonia

Corresponding author:
Besar Abdiu

Received:
March 3, 2025

Revised:
May 29, 2025

Accepted:
September 17, 2025

Published:
November 28, 2025

Citation:
Abdiu, B. et al. Implementation of a substructure method to analyse soil-structure interaction at an existing 10-storey reinforced concrete building. *Advances in Civil and Architectural Engineering,* 2025, 16 (31), pp. 220-234. https://doi.org/10.13167/2025.31.13

ADVANCES IN CIVIL AND ARCHITECTURAL ENGINEERING (ISSN 2975-3848)

Faculty of Civil Engineering and Architecture Osijek
Josip Juraj Strossmayer University of Osijek
Vladimira Preloga 3
31000 Osijek
CROATIA

Abstract:
In earthquake-resistant design, structures are usually assumed to be fixed at their bases. Although in some cases this assumption may be realistic, in other cases it is neither reasonable nor conservative and the consequences can be significant. Many investigations of soil-structure interaction (SSI) in recent decades have been related to prototype frame buildings. On the other hand, relatively few investigations of SSI have considered existing structures and structures of mixed systems. This work investigates SSI in a 10-storey reinforced concrete structure built in the 1970s in Ohrid, North Macedonia. The building is part of Ohrid's 3D seismic network and is instrumented in the soil profile, foundation structure and two storeys. Thus, it provides an ideal example to investigate SSI. The interface between the soil and the structure is substituted with springs to consider the flexibility of the connection between the soil and the structure. The results of the flexible base structure are provided in terms of the reduced demands (reduced response spectra and the elongation of fundamental vibration period) and these are compared with the fixed base counterparts. The findings of this study contribute to a better understanding of SSI effects in dual systems and provide valuable insights for more accurate seismic design practices incorporating SSI.

Keywords:
soil-structure Interaction; RC structure; flexible base; fixed base

1 Introduction

Usually, when designing structures, it is assumed that they are rigidly attached to the soil beneath, and fixed supports are assigned to the base of the mathematical model. The design of the foundations is then carried out using the forces acting on the fixed support. Although common in practice, this simplified approach may lead to discrepancies in seismic response predictions [1]. This simplification was justified in the past given the lack of computerized tools and computational capacity. Nowadays, when computational effort is no longer a limitation, the interface between the soil and structure should and, in some cases, must be considered more realistically through by implementing soil–structure interaction (SSI). Although computational capabilities have advanced in recent decades, validating SSI models using real-world data remains challenging. Recent studies have demonstrated that neglecting SSI effects can lead to both excessively radical and overly conservative design depending on the structural system and soil conditions [2]. Soil-structure interactions do not manifest in the same way in all types of structures. For example, its effects are more pronounced in structures with larger lateral stiffness. Variations in SSI effects have been documented through extensive parametric studies [3]. In fact, situations in which SSI is likely to be significant depend not only on the lateral stiffness of the structure but also on the stiffness of the soil itself. To estimate the significance of SSI on buildings, the so-called structure-to-soil stiffness ratio is used, as discussed in Section 3. This ratio has been established as a key parameter in determining the importance of SSI effects [4]. This stiffness ratio also depends on the foundation system which forms the connection between the soil and the superstructure. Thus, soil-structure interaction is a complex problem that depends on many factors, and its effects are not readily apparent.

Many studies have been conducted in recent decades to understand the consequences of soil-structure interaction on building structures. Moment-resisting frames made of reinforced concrete or structural steel resting on any kind of foundation system are among the most investigated structural systems. For example, Wani et al. [5] studied the effects of a multistorey building resting on a mat foundation. The effects of soil flexibility were demonstrated by using different types of soil categories. Samali, Fatahi, and Tabatabaiefar [6] performed a nonlinear time-history analysis in FLAC2D to compare the lateral displacement of a fixed-base reinforced concrete moment-resisting frame building with those of its flexible-base counterpart. Their research has shown that the interaction between structures and the soil can change the level of performance of a building from ‘life safe’ to ‘near collapse.’ Similar results have been demonstrated by comparing inter-storey drifts [7]. They conducted an experimental study to validate their work [8]. Brandis, Kraus and Petrovčič [9] have studied the nonlinear behaviour of a steel structure considering SSI. The building considered consisted of braced frames in one direction and moment-resisting frames in the orthogonal direction. They demonstrated that the N2 method can also be implemented when SSI is considered because the investigated structure vibrated predominantly in the first mode.

Carbonari Dezi and Leoni [10] performed a linear time-history analysis to study the influence of SSI on a dual wall-frame structure resting on pile foundations. A similar structure was used to extend their work to nonlinear stages [11]. The results of these studies have generally shown that SSI tends to increase deformations. On the other hand, regarding force quantities, SSI tends to decrease forces in walls while increasing them in frames. Similar behaviour has also been confirmed in dual wall-frame structures in other investigations [12; 13]. Emami and Halabian [14] showed that ductility demand decreases with increasing soil flexibility.

Generally, the volume of research on dual wall-frame structures is not comparable to that of work on moment-resisting frames [15]. Considering that the behaviour of mixed-type structural systems such as dual wall-frame systems is less predictable than that of frame structures, it is clear that there is still room to improve on the limitations of previous studies.

The building considered in this work is a good example for studying soil-structure interaction. The fact that the location of the building in question is a part of the seismic network of Ohrid, makes this work even more interesting. In particular, the main advantage of this work is that the building considered here is instrumented with the soil beneath down to the bedrock. One

of the main advantages of working with an instrumented building is the ability to use real recorded data directly for numerical model validation. In the numerical model, the recorded acceleration at the building's foundation (e.g., from the 2021 Ohrid earthquake) is applied as input motion. By applying this excitation, the model simulates the structural response of the building in that situation, such as accelerations at various characteristic points. These numerical results can then be compared with the data recorded by the instruments installed at the corresponding locations within the building, to provide a basis for evaluating the accuracy and validity of the model.
In this study, the application of SSI procedures is demonstrated in a 10-storey reinforced concrete building resting on pile foundations. First, the stiffness and damping coefficients were estimated by using the procedures proposed in [4]. The values obtained for the springs and dashpots were then applied to a flexible-base model. Finally, the dynamic quantities of the flexible-base model were compared with those of its fixed-base counterpart. In this study, only a linear elastic analysis was carried out, in which both the superstructure and the uniaxial soil springs were modelled elastically.

2 Building description and modelling

The building considered (referred to here as the Tower) is a 10-storey RC structure with an overall height of 36 m. The building location is one of the four instrumented locations of the Ohrid 3D seismic network, installed in the 80s by the Institute of Earthquake Engineering and Engineering Seismology and the United States Geological Survey. The building was constructed at the end of 70s. The structural system of the building is dual in one direction and a pure frame in the orthogonal direction. Its foundation consists of groups of piles joined at their tops with pile caps and interconnected with grade beams. Walls are supported on grade beams, which in turn transfer the loads to the piles beneath, which are distributed along the length of the grade beams. Further information can be found in the IZIIS report No. 2021-61 [16] and IZIIS report No. 2021-62 [17]. In the subsequent text, only the information needed to model the foundation is introduced.

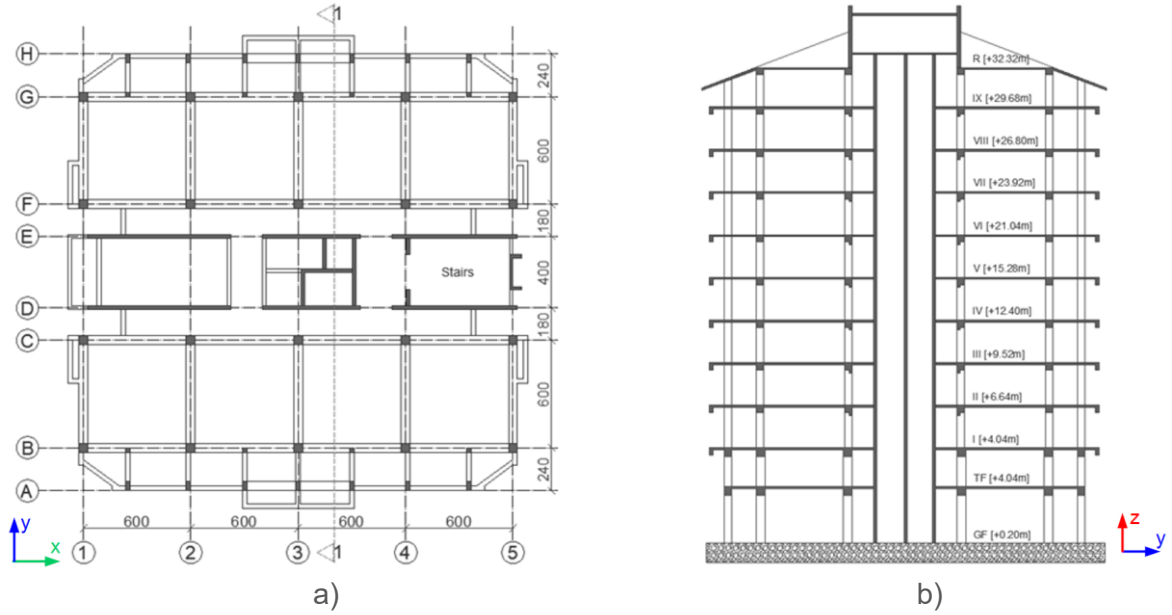

a) b)

Figure 1. Analysed building: a) characteristic plan view; b) characteristic section

The analysed structure is a mixed-use building with the ground floor designated for commercial use and the upper levels for residential purposes. The building has an approximately square

plan measuring 24,0 meters by 24,4 meters and consists of eleven levels, including a ground floor, a mezzanine, eight standard stories, and an attic. The ground floor has a height of 3,84 meters, whereas the mezzanine is 2,60 meters high. The remaining stories have a uniform height of 2,88 meters. Figure 1 presents the characteristic plan and section of the building [18-20].

The structure features a mixed reinforced concrete structural system with square and rectangular columns that gradually decrease in cross-sectional dimensions as they ascend from the ground floor. Reinforced concrete diaphragms are positioned in the central part of the structure along one of its axes of symmetry. The space for the staircase is allocated between these diaphragms at one end of the building. All the structural elements were assigned elastic material properties. The frame elements were modelled as line elements, while the walls and floors were modelled using shell elements. Uncracked sections were assigned to all elements. Figure 2 shows a photograph of the building.

Figure 2. Photo of the analysed building

3 Modelling of the foundation structure

The foundation system consists of piles with solitary footings interconnected by foundation beams (ties) in both orthogonal directions. The relatively thin slab on grade also contributes to

interconnect the individual footings. Each solitary footing rest on four piles, except for the end footings, which are supported by three piles each. The diaphragms are also founded on piles supported by a strip foundation. The gross foundation area is considered to calculate the parameters required for soil and foundation modelling even though the foundation system consists of solitary footings, piles, tie beams, and the slab on grade. This is justified by the fact that the stress bulbs of the foundation beams and pile caps overlap at shallow depths.

3.1 Average effective shear wave velocity

The shear wave velocity over the soil profile was constructed from the IZIIS report No. 2021–62 [17] (Figure 3). The average effective shear-wave velocity was calculated using the following expression [4]:

$$V_{s,avg} = \frac{z_p}{\sum_{i=1}^{n}\left(\frac{\Delta z_i}{\left(V_{s,F}(z_i)\right)_i}\right)} \quad (1)$$

The calculated values of the average effective shear wave velocity with and without considering the overburden pressure due to the added weight of the structure are listed in Table 1.

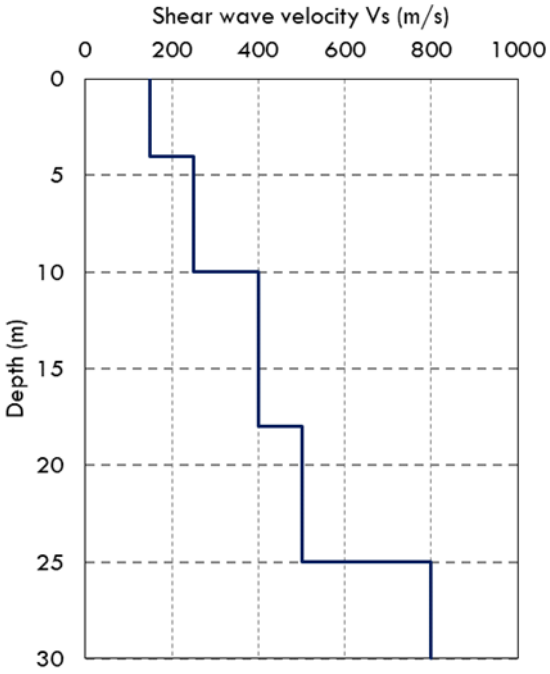

Figure 3. Shear wave velocity over the soil profile

Table 1. Calculation of average effective shear wave velocity

Vibration mode	z_p (m)	Depth range		$V_{s,avg}$ (m/s)	$V_{s,F,avg}$ (m/s)
		from	to		
x (translation)	12,30	1,7	14,0	249,32	311,25
y (translation)	12,30	1,7	14,0	249,32	311,25
z (translation)	12,30	0,0	14,0	230,77	303,78
xx (rocking)	12,30	0,0	14,0	230,77	303,78
yy (rocking)	12,30	0,0	14,0	230,77	303,78

3.2 Soil-structure Interaction

The soil-structure interaction phenomenon becomes significant in cases in which [4]:

$$\frac{h}{v_s \cdot T} > 0{,}1 \tag{2}$$

Using the above expression, a value of 0,13 was obtained for the considered building, which means that the soil-structure interaction is significant and should be considered in the structural analysis. However, this is only true for the stiffer direction of the structure (with a fundamental period of 0,65 sec). In the orthogonal direction, the fundamental period is longer (T=1,22 sec), and the left-hand side of the above inequality gives a value of 0,065, which is smaller than 0,1; hence, the SSI is not significant in this direction.

3.3 Horizontal stiffness and damping

The calculation of spring stiffness (k_j) and damping ratios (c_j) for each degree of freedom is carried out in this section. For convenience, the parameters required to calculate k_j and c_j are listed in Table 2. The foundation spring and dashpot quantities for each degree of freedom can then be calculated according the [4]. The calculated values are provided in Table 3.

Table 2. Parameters for calculation of k_j and c_j

Vibration mode	$V_{s,F,avg}$ (m/s)	G_o (MPa)	G (MPa)	K^*_{sur} (kN/m; kN-m/rad)	η*	a_0	α	β_{sur}	β_{emb}
x (transl.)	311,25	178,7	178,7	11897766	---	0,382	1,00	0,141	---
y (transl.)	311,25	178,7	178,7	11897766	---	0,382	1,00	0,141	---
z (vertical)	303,78	170,3	170,3	14061802	1,10	0,391	1,00	---	0,227
xx (rocking)	303,78	170,3	170,3	1810561783	1,16	0,391	0,96	---	0,014
yy (rocking)	303,78	170,3	170,3	1810561783	1,16	0,391	0,96	---	0,014
*Calculated using expression given by Pais and Kausel [21]									

Table 3. Spring and dashpot quantities

Vibration mode	k_j	c_j
x (transl.)	11897766 kNm	3359326 kNs/m
y (transl.)	11897766 kNm	3359326 kNs/m
z (vertical)	15483487 kNm	728326 kNs/m
xx (rocking)	2019551980 kNm/rad	57849992 kNs/m/rad
yy (rocking)	2019551980 kNm/rad	57849992 kNs/m/ad

3.4 Vertical stiffness and damping

As listed in Table 3, the stiffness and damping quantities are intended to cover the whole footprint of the building. However, to model the soil reactions properly, springs and dashpots should be distributed over the building footprint and normalized by the tributary areas of the columns and walls as calculated with the help of the Tribby3d software [22]. On that point, the dots shown in Figure 4 represent a vertical structural member (a column or wall), whereas the zones enclosed by the solid black lines denote the tributary areas of the considered columns or walls. Thus, the vertical stiffness of the soil would be reproduced. However, the vertical stiffness of the soil is not uniform over the whole building footprint due to the rocking. Rather, it tends to increase at the edges and corners of the footprint. The opposite is true for dashpot coefficients. The correction factors given in [4] were applied to consider these differences, that is, to increase the vertical stiffness at edges and corners and to reduce the damping ratios at the same locations. The calculated values are shown in Table 4 along with the corrected values and are schematically presented in Figure 4.

Table 4. Corrected values of vertical stiffness and damping coefficients

Zone	k_z^i (kN/m^3)	c_z^i (kNs/m^3)
z	25586	1204
yy	77358	3563
xy	77358	3563
xx	77358	3563

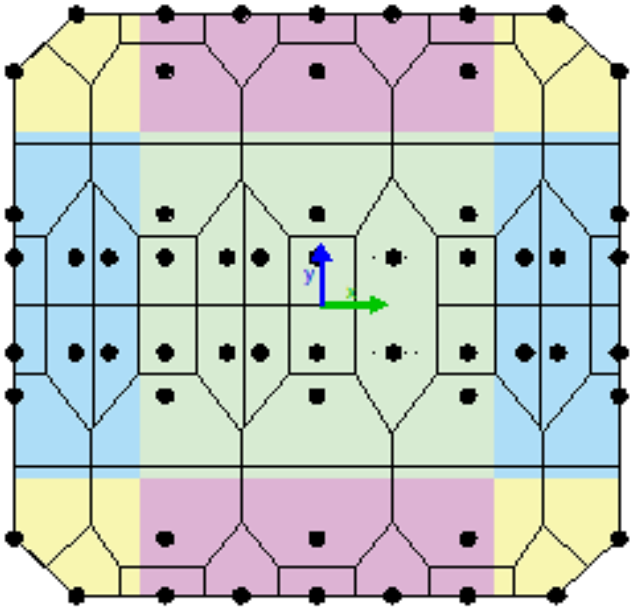

Figure 4. Distribution of stiffness and damping intensities over the building footprint

It may easily be noted that the edge springs have the same intensity in both orthogonal directions. This is the case due to the bisymmetric shape of the building footprint. Corner springs also have the same intensity (as the average value of two identical numbers).

3.5 Contribution from pile groups

In our case, both vertical and lateral loads originating from the superstructure should be resisted by shallow and deep foundations. Hence, the piles are subjected to both axial and lateral loads. However, their active lengths differ depending on the corresponding degree of freedom. This difference is also reflected in the calculation of subsequent parameters such as the average shear wave velocity, shear modulus, static pile stiffness, and so forth. The calculated values of pile stiffness and damping parameters are listed in Table 5.

Table 5. Calculation of average effective shear wave velocity

Vibration mode	Group of piles	L_a (m)	$V_{s,F,avg}$ (m/s)	G (MPa)	K_j^P (MN/m)	k_j^G	β_j
x, y (transl.)	(2 x 2)	3,5	264,46	50,14	184,57	0,65	0,12
z (transl.)	(2 x 2)	9,0	380,10	188,67	886,17	0,60	0,12

The stiffness of pile group under a pile cap is calculated with the following expression:

$$k_{piles}^G = n_{piles} \cdot K_j^P \cdot k_j^G \quad (3)$$

We note that the same group efficiency factor (k_j^G) was used for both the group with 3 piles and that with 4 piles. The contributions of other piles were considered as acting individually.

3.6 Distribution of springs to foundation nodes

The foundation structure of the building was modelled with a total number of 58 nodes (Figure 5). Only 16 of them contributed to the horizontal stiffness in the x-direction and 18 to that in the y-direction. Half were placed on one edge and the other half on the opposite edge. In other words, the springs contributing to the horizontal stiffness were distributed along the perimeter of the building footprint. On the other hand, all 58 nodes are engaged in the vertical stiffness of the foundation. However, as noted above, their intensity depends on the tributary area and on the spring location within the building footprint, which means that the vertical stiffness is not constant. The overall horizontal stiffness of the building foundation is the sum of the horizontal pile stiffness and the horizontal shallow foundation stiffness.
As mentioned above, the intensity of the springs differs because the vertical stiffness is not a constant value over the entire building footprint, which means that it depends on the number of piles and the location under consideration. Thus, this value was calculated separately for each node.

3.7 Foundation modelling

In IZIIS report no. 2021-61 [16], the mathematical model of the superstructure with a fixed base was modelled using the SAP2000 software package [23]. The same model is used here, with some changes at its base. In particular, the fixed supports are removed and the foundation is modelled using springs with intensities as calculated in the previous sections. The distribution of these springs is shown in Figure 5. Note that only uniaxial springs are used in the three orthogonal directions of the building. The rocking of the foundation was modelled with corrected values of the vertical springs at the edges and corners of the foundation, while the torsional DOF is considered fixed due to the considerable stiffness provided by the tie beams and the slab on grade. In other words, the scheme 3 given in NIST [4], with vertical and horizontal springs, was used to model the interface between the soil and the structure. This scheme is reproduced Figure 6.

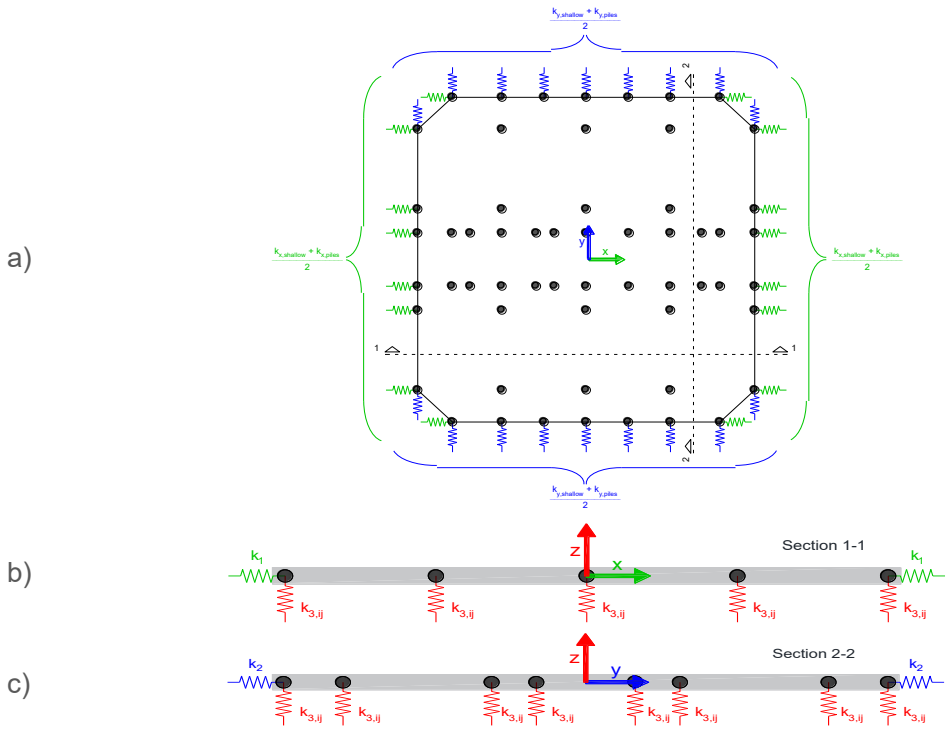

Figure 5. Distribution of horizontal and vertical springs: a) plan view; b) section 1-1; c) section 2-2

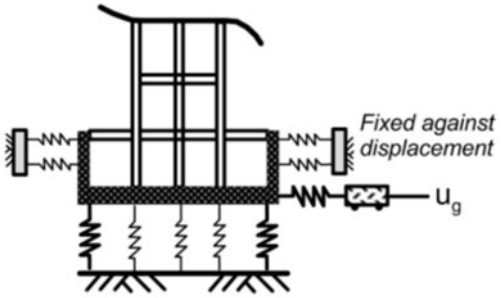

Figure 6. Modelling the interface between the soil and the structure [4]

4 Analysis of the flexible-base model

This section presents an analysis of the Tower building with a modified foundation, i.e., a replacement of the fixed supports with elastic springs. The values of the vertical and horizontal springs calculated in the previous section were assigned to the building following the pattern illustrated in Figure 6. A three-dimensional view of the model is shown in Figure 7. In this section, the effects of base slab averaging, period elongation due to the flexible base, and foundation damping were analysed.

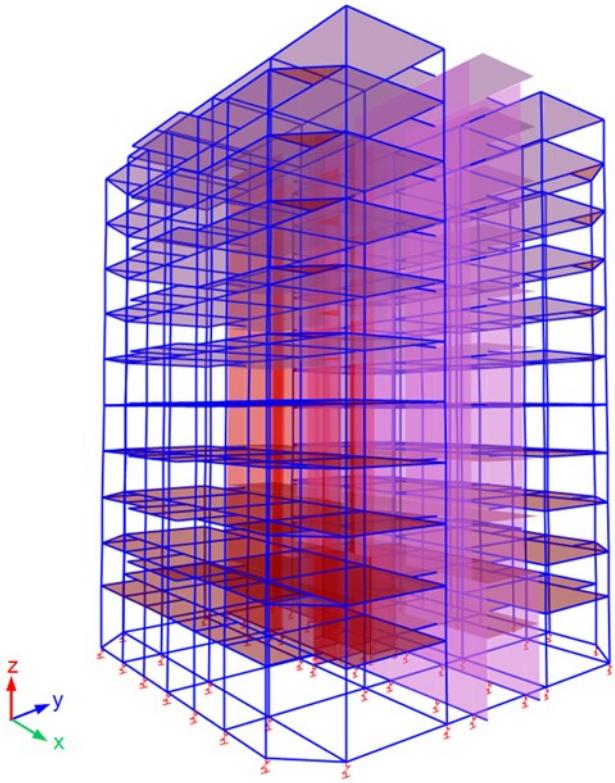

Figure 7. View of the 3D flexible model

4.1 Base slab averaging

According to ASCE/SEI 7-16 [24], the effect of base slab averaging can be determined based on the average seismic shear wave velocity and foundation base area, although it depends on additional factors such as building geometry, frequency content, and the spatial variability of the earthquake wave field. In fact, this standard allows the base slab averaging to be accounted for in the design only if the average seismic shear wave velocity value is within limits: 200 m/s ≤ v_s ≤ 500 m/s [24].

The factor reducing the response spectrum (RRS_{bsa}) is a function of the period T. Up to the period of 0,2 sec, the value of this factor is constant and for larger periods its value increases. The calculations for the whole spectrum were carried out in a spreadsheet. In Figure 8, the resulting values of RRS_{bsa} are given graphically.
Of note, the spectral reduction is not linked to particular parameters which may be applicable only for ASCE/SEI 7-16 spectra. Rather, it is a ratio of reduced and unreduced response spectra. Thus, the RRS_{bsa} coefficient may be used to reduce the EC8 Type 1 elastic response spectrum ordinates for an acceleration of 0,3g, 5 % damping, and soil class C [25]. Figure 9 shows both the unreduced and reduced response spectra. It may be clearly observed that the largest reductions in the spectrum ordinates occur in the interval 0 to 0,2 sec and, as the period increases, the reduction diminishes. Finally, the base slab averaging effect is negligible for this building, even for the ordinates not corresponding to the fundamental vibration period of the structure.
The negligible effect of base slab averaging in reducing the linear elastic spectrum is shown clearly in Figure 9. However, this finding should not be generalised to other methods of analysis. For example, if a nonlinear time–history analysis is to be performed on a flexible-base structure, the base slab averaging effect may significantly affect the target spectrum or the individual earthquake records considered for this type of analysis.

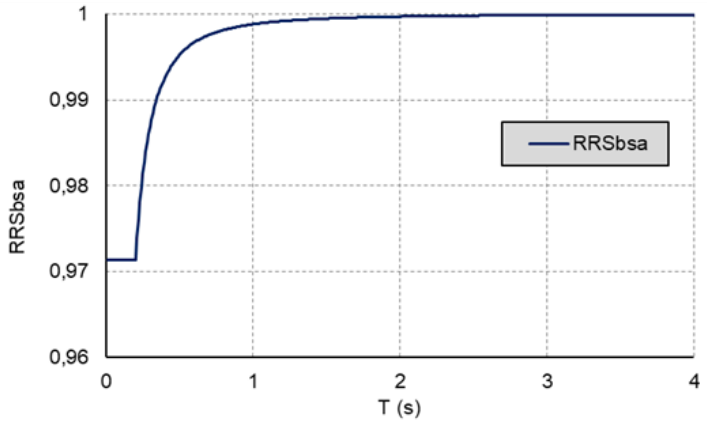

Figure 8. Variation of RRS_{bsa} with period

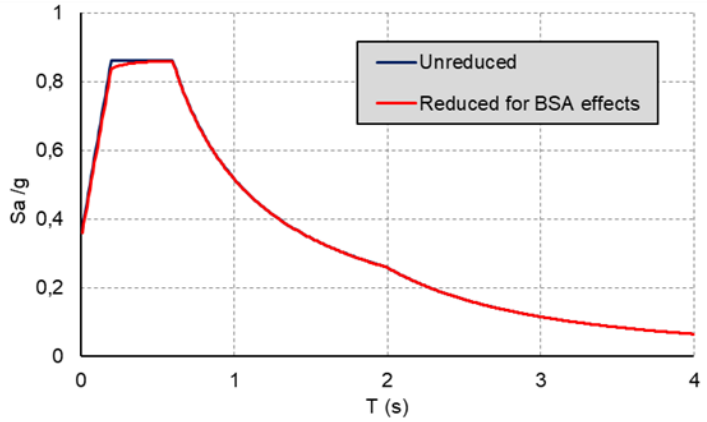

Figure 9. Unreduced and reduced response spectra for BSA effects (EC8 Type 1 response spectrum for acceleration of 0,3g, soil class C, and 5 % damping)

4.2 Period elongation

The substitution of fixed supports with springs at the base of the original model resulted in an overall increase in the structural flexibility. The elongated periods (T') for both orthogonal

directions together with their fixed-base counterparts (T) are shown in the table below. Also, the rightmost column shows the ratio of the elongated periods to the periods of the structure with fixed base (T'/T). As expected, the consideration of the SSI mostly affects the stiffer direction of the structure.

Table 6. Calculation of average effective shear wave velocity

	T	T'	T'/T
X - direction	1,218 sec	1,325 sec	1,088
Y - direction	0,653 sec	0,745 sec	1,142

The elongation of the fundamental period can have a favourable or unfavourable effect on the seismic behaviour of the structure, depending on whether the fundamental period is on the acceleration-, velocity-, or displacement-sensitive regions. To visualise the consequences of this period shift, the acceleration elastic response spectrum and its displacement counterpart are shown in Figures 10 and 11, respectively. In addition, both the 'original' and the elongated periods are shown for both orthogonal directions.
Because the fundamental periods of the structure lie at the beginning of the velocity-sensitive region, the acceleration ordinate decreases and the displacement ordinate increases. This is true in both directions. Again, it is clear that the direction most affected by the period elongation is the stiffer one (the Y-direction).

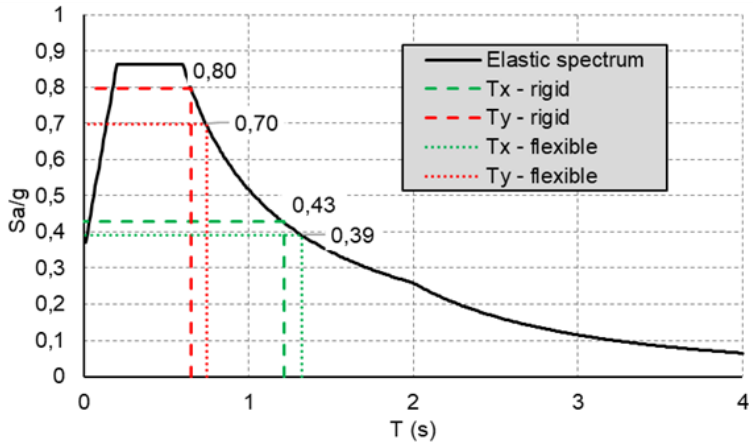

Figure 10. Period elongation in the acceleration spectrum

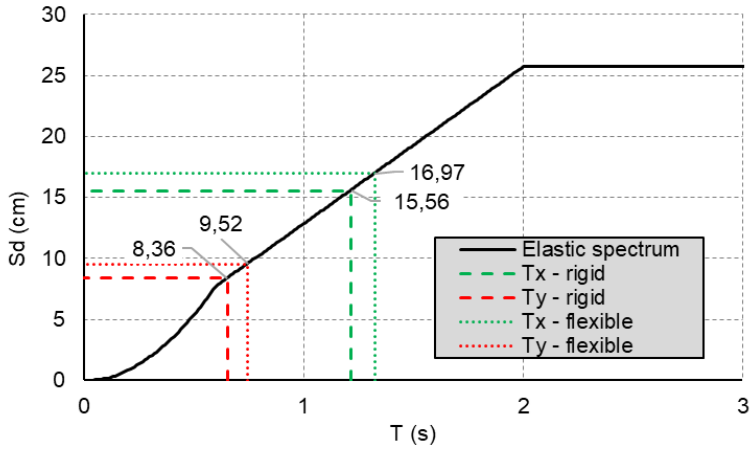

Figure 11. Period elongation in the displacement spectrum

4.3 Foundation damping

The procedure for calculating foundation damping is given in section 19.3 of ASCE/SEI 7-16 [24]. However, the procedure cannot be applied if the foundation of the structure is classified as falling into one of the groups given in Section 19.3.1 of ASCE/SEI 7-16. One of these groups includes structures with deep foundations, which means that the procedure does not apply in our case. However, as for the base slab averaging, foundation damping was calculated for our structure simply to provide some insight. The obtained value of the effective damping ratio for the soil-structure system is 0,059. This is taken as the governing value because it is smaller than 0,2.

5 Conclusions and recommendations

In this study, the procedure for considering the soil-structure interaction was demonstrated for a real structure located in Ohrid, North Macedonia. From this work, the following conclusions can be drawn:

- The SSI has a larger effect in the Y-direction of the building than in the X-direction. In other words, the stiffer direction is more sensitive to base flexibility.
- The effects of base slab averaging are negligible for the building considered.
- The substitution of fixed supports with springs resulted in an increase in flexibility (period elongation) which affected the structural response and the response spectrum used for the design. The larger the elongation period, the more the design is affected.
- The decrease in the design acceleration spectrum ordinate owing to the period elongation is usually accompanied by an increase in the design displacement spectrum ordinate. Thus, although the design forces are reduced, there is an increase in the lateral displacement and inter-storey drifts, which may change the performance level of the building.

Because there are no instructions in European codes on how to consider SSI effects, a combination of ASCE/SEI 7-16 procedures and Eurocode 8 parameters has been used in this work to describe the quantities of interest. Thus, the following recommendations are provided to suggest some directions for future research:

- Develop formulations for SSI quantities in terms of Eurocodes. The main challenge in matching ASCE-based methods to the Eurocode criteria lies in the empirical equations for reducing the base shear force due to the consideration of SSI. These equations are based on the design spectrum quantities and on the response modification coefficients, which are defined differently in the two codes. The application of SSI in the design of structures in accordance with European codes must be preceded by a harmonisation of these quantities.
- Compare the parameters given in both standards more explicitly and describe a procedure for considering of SSI in terms of European standards.
- Define the lower-bound limit for reduction of base shear when SSI is considered in the Eurocode 8 procedure.
- Analyse the nonlinear response of this structure with a flexible foundation and compare it with its fixed-foundation counterpart. In this context, an adequate nonlinear model (e.g., a baseline or rigid bathtub model) that captures the nonlinear properties of both the superstructure (nonlinear hinges) and the underlaying soil (nonlinear springs and dashpots) should be adopted.
- Include the higher modes. The present study focused on fundamental vibration modes in each orthogonal direction. The effects of higher modes may alter the dynamic characteristics of the structure.

Indices and symbols

Symbol	Description	Unit
a_0	Dimensionless frequency	-
c_j	Dashpot coefficient	kNs/m; kNs/m/ad
c_z^i	Vertical dashpot intensity	kNs/m^3
G	Reduced shear modulus of the soil accounting for seismic events causing large strain in the soil	MPa
G_o	Maximal (small-strain) shear modulus of the soil	MPa
h	Effective height of the structure (two-thirds of the actual height)	m
K^*_{sur}	Static stiffness of shallow foundation at the ground surface	kN/m; kN-m/rad
k^G_{piles}	Pile group stiffness intensity	MN/m
k_j	Spring coefficient	kN/m;kN-m/rad
k_j^G	Pile group efficiency factor	-
K_j^P	Pile static stiffness	MN/m
k_z^i	Vertical stiffness intensity	kN/m^3
L_a	Active pile length	m
n_{piles}	Number of piles connected by a pile cap	-
RRS_{bsa}	Response spectrum reduction factor accounting for base slab averaging effects	-
T	Fundamental vibration period of the fixed-base structure	s
T’	Fundamental vibration period of the flexible-base structure	s
v_s	Shear wave velocity of the soil	m/s
$V_{s,avg}$	Average effective shear wave velocity	m/s
$V_{s,F}(z_i)$	Corrected shear wave velocity of a layer to account for overburden pressures due to the added weight of the structure	m/s
$V_{s,F,avg}$	Corrected average effective profile velocity to account for overburden pressures due to the added weight of the structure	m/s
z_p	Effective profile depth	m
α	Dimensionless factor, function of dimensionless frequency	-
β_{emb}	Radiation damping ratio due to the embedment effects	-
β_j	Pile group damping ratio	-
β_{sur}	Radiation damping ratio at the ground surface	-
Δz_i	Soil layer thickness	m
η*	Embedment correction factor for static stiffness of rigid footings	-

References

[1] Mylonakis, G.; Gazetas, G. Seismic soil-structure interaction: beneficial or detrimental? *Journal of Earthquake Engineering*, 2000, 4 (3), pp. 277-301. https://doi.org/10.1080/13632460009350372

[2] Kim, D. S.; Yoon, J.; Cho, W.; Lee, J. Evaluation of Seismic Performance and Soil-Structure Interaction (SSI) for Piloti-Type Buildings considering Korean Geotechnical Conditions. *Advances in Civil Engineering*, 2021, 2021 (1), 7876389. https://doi.org/10.1155/2021/7876389

[3] Pitilakis, D. et al. Large-scale field testing of geotechnical seismic isolation of structures using gravel-rubber mixtures. *Earthquake Engineering & Structural Dynamics*, 2021, 50 810), pp. 2712-2731. https://doi.org/10.1002/eqe.3468

[4] U.S. Department of Commerce, National Institute of Standards and Technology. NIST GCR 12-917-21. Soil-Structure Interaction for Building Structures (NEHRP). USA: NIST GC; 2012.

[5] Wani, M. F.; Vemuri, J.; Rajaram, C.; Babu R, V. D. Effect of soil structure interaction on the dynamic response of reinforcced concrete structures. *Natural Hazards Research*, 2022, 2 (4), pp. 304-315. https://doi.org/10.1016/j.nhres.2022.11.002

[6] Samali, B.; Fatahi, B.; Tabatabaiefar, R. H. Seismic behaviour of concrete moment resisting buildings on soft soil considering soil-structure interaction. In: *Incorporating Sustainable Practice in Mechanics and Structures of Materials*, Fragomeni, S.; Venkatesan, S. (eds.). CRC Press; 2010, pp. 407-412.

[7] Tabatabaiefar, S. H. R.; Fatahi, B.; Samali, B. Seismic Behavior of Building Frames Considering Dynamic Soil-Structure Interaction. *International Journal of Geomechanics*, 2013, 13 (4), pp. 409-420. https://doi.org/10.1061/(ASCE)GM.1943-5622.0000231

[8] Tabatabaiefar, S. H. R.; Fatahi, B.; Samali, B. Numerical and Experimental Investigations on Seismic Response of Building Frames under Influence of Soil-Structure Interaction. *Advances in Structural Engineering*, 2014, 17 (1), pp. 109-130. https://doi.org/10.1260/1369-4332.17.1.109

[9] Brandis, A.; Kraus, I.; Petrovčič, S. Nonlinear Static Seismic Analysis and Its Application to Shallow Founded Buildings with Soil-Structure Interaction. *Buildings*, 2022, 12 (11), 2014. https://doi.org/10.3390/buildings12112014

[10] Carbonari, S.; Dezi, F.; Leoni, G. Linear soil-structure interaction of coupled wall-frame structures on pile foundations. *Soil Dynamics and Earthquake Engineering*, 2011, 31 (9), pp. 1296-1309. https://doi.org/10.1016/j.soildyn.2011.05.008

[11] Carbonari, S.; Dezi F.; Leoni, G. Nonlinear seismic behaviour of wall-frame dual systems accounting for soil-structure interaction. *Earthquake Engineering & Structural Dynamics*, 2012, 41 (12), pp. 1651-1672. https://doi.org/10.1002/eqe.1195

[12] Hutchinson, C. T.; Raychowdhury, P.; Chang, B. Nonlinear structure and foundation response during seismic loading: dual lateral load resisting systems. In: Proceedings of the 8th US National Conference on Earthquake Engineering. April 18-22, 2006, San Francisco, USA, Earthquake Engineering Research Institute; 2006, 320.

[13] Katrangi, M.; Memarpour, M. M.; Yakhchalian, M. Assesment of the Seismic Performance and the Base Shear Contribution Ratios of the RC Wall-frame Dual System Considering Soil-Structure Interaction. *Journal of Earthquake Engineering*, 2022, 26 (10), pp. 5290-5317. https://doi.org/10.1080/13632469.2021.1871678

[14] Emami A.; Halabian, A. M. Seismic response assessment of reinforced concrete structures based on displacement, force and energy criteria, considering soil-structure interaction. *Australian Journal of Structural Engineering*, 2020, 21 (1), pp. 64-93. https://doi.org/10.1080/13287982.2019.1706700

[15] Bapir, B.; Abrahamczyk, L.; Wichtmann, T.; Prada-Sarmiento, L. F. Soil-structure interaction: A state-of-the-art review of modelling techniques and studies on seismic response of building structures. *Frontiers in Built Environment*, 2023, 9. https://doi.org/10.3389/fbuil.2023.1120351

[16] Institute of earthquake engineering and engineering seimology. IZIIS Report No. 2021-61, 2021a.

[17] [17] Institute of earthquake engineering and engineering seimology. IZIIS Report No. 2021-62, 2021b.

[18] Bojadjieva, J. et al. Seismic site investigation and structural amplification based on geotechnical and structural health monitoring. In: *Data-Centric Structural Health Monitoring: Mechanical, Aerospace and Complex Infrastructure Systems*, Noori, M. et al. (eds.). De Gruyter; 2023, pp. 1-28. https://doi.org/10.1515/9783110791426-001

[19] Bogdanovic, A. et al. Structural Health Monitoring as a Tool toward More Resilient Societies. In: Automation in Construction toward Resilience, Farsangi, E. N. et al. (eds.). Boca Raton: CRC Press; 2023, pp. 199-222. https://doi.org/10.1201/9781003325246-11

[20] Shoklarovski, A. et al. Experimental investigation of eleven stories building by ambient vibration method. In: *18th World Conference on Earthquake Engineering (WCEE2024)*. Milan, Italy 2024; 2024.
[21] Pais, A.; Kausel, E. Approximate formulas for dynamic stiffnesses of rigid foundations. *Soil Dynamics and Earthquake Engineering*, 1988, 7 (4), pp. 213-227. https://doi.org/10.1016/S0267-7261(88)80005-8
[22] Tribby3d. Structural loading software Tribby3d. Accessed: November 27, 2025. Available: https://tribby3d.com
[23] Computers & Structures, Inc. CSI. SAP2000 Version 23.3.0. Accessed: November 27, 2025. Available: https://www.csiamerica.com
[24] American Society of Civil Engineers. ASCE/SEI 7-16. *Minimum Design Loads and Associated Criteria for Buildings and Other Structures*. USA: ASCE; 2017. https://doi.org/10.1061/9780784414248
[25] European Committee for Standardization. *Eurocode 8: Design of structures for earthquake resistance — Part 1: General rules, seismic actions and rules for buildings*. Brussels; 2004.